International Scholarly Research Network
ISRN Renewable Energy
Volume 2012, Article ID 859519, 5 pages
doi:10.5402/2012/859519

Research Article

Design and Simulation of Multiquantum-Well AlGaAs/GaAs Single Junction Solar Cell with Back Surface Reflector

Hamid Fardi

Department of Electrical Engineering, University of Colorado Denver, P.O. Box 133363, Denver, CO 80217, USA

Correspondence should be addressed to Hamid Fardi, hamid.fardi@ucdenver.edu

Received 25 April 2012; Accepted 4 July 2012

Academic Editors: D. C. Martins and X.-F. Wang

This paper reports on the design and simulation of a multiquantum Well (MQW) AlGaAs/GaAs single p-i-n junction cell with a Distributed Bragg Reflector (DBR) placed at back surface. The DBR structure reflects the part of the spectrum that benefits from absorption in the AlGaAs MQW structure, while being transparent to the IR spectrum. The addition of a DBR allows for a possible second bottom cell junction to be placed beneath the DBR in series with the MQW single cell for an additional efficiency enhancement. The efficiencies and short-circuit currents for the AlGaAs MQW cell with and without DBR are simulated. An energy balance equations model coupled with drift-diffusion equations is solved in heterojunction p-i-n with embedded quantum wells to model hot electron effects. The current-voltage characteristics of an MQW single junction AlGaAs/GaAs p-i-n solar cell structure were compared with measured data. The efficiencies and short-circuit currents of an optimized cell with and without DBR are simulated. Results obtained show improvement in short circuit current and efficiency when both MQW and DBR were used. Simulation results predict an efficiency of about 28.4% for the MQW AlGaAs-DBR single p-i-n junction photovoltaic cell under the presence of both radiative and nonradiative recombination mechanisms.

1. Device Design

The single junction structure proposed consists of an *AlGaAs/GaAs* MQW top cell and an *AlAs/GaAs* DBR reflector at the back. Incorporating GaAs quantum wells in the intrinsic region of a *p-i-n* $Al_xGa_{1-x}As$ solar cell can increase the efficiency of the single bandgap baseline cell as it is reported by several investigators [1–4].

Simulations of solar cells are carried out by modeling an energy balance hot carrier model. For the light illumination an AM 1.5 solar spectrum condition with input power equal to 100 mW/cm^2 is used.

The optimized device is similar to the work published by others [5], where the optimization was carried out by simulation of devices with various geometrical and electrical parameters. The geometry of layers was changed by altering their thicknesses. The doping concentration and bandgap energy of particular material were considered as the main electrical parameters. For p-i (MQW)-n solar cell simulations parameters such as the widths of the wells and barriers, the depth of wells with a constant value of intrinsic region width, the number of wells in the intrinsic layer, doping concentration of emitter layer, width and doping concentration of the base layer, width of separation layers, and Al fraction in the window layer were changed. Devices which have achieved the highest value of conversion efficiency were classified to the next step of optimization [6, 7]. The optimized structure of the MQW solar cell is shown in Figure 1. The device considered contains two 15 nm wide *GaAs* wells and 10 nm wide $Al_{0.1}Ga_{0.9}As$ barriers. Two, 20 nm wide emitter layer and 1000 nm base layer are applied, and the window layer is composed of $Al_{0.9}Ga_{0.1}As$. The cap layer application is required due to high contents of Al in window layer. Figure 2 shows the energy band diagram of the *AlGaAs/GaAs* MQW cell without the addition of the DBR.

The DBR structure is formed from multiple layers of alternating materials with varying refractive index [8]. Each layer boundary causes a partial reflection of an optical wave. The refractive index and the thicknesses of *GaAs* and *AlAs* layers must be properly chosen for a particular wavelength. Here, it is desirable to reflect photons which have energies in the range between 1.4 ev and 1.6 ev. The refractive indexes

Top electrode		
$P+$ GaAs	Cap layer	100 nm, $N_a = 4e18$
$P+$ $Al_{0.9}Ga_{0.2}As$	Window layer	10 nm, $N_a = 4e18$
$P+$ GaAs	Emitter	100 nm, $N_a = 4e18$
$Al_{0.1}Ga_{0.8}As$	Spacer layer	25 nm
$Al_{0.1}Ga_{0.8}As$	Barrier	10 nm
GaAs "i"	Well	15 nm
$Al_{0.1}Ga_{0.8}As$	Barrier	10 nm
GaAs "i"	Well	15 nm
$Al_{0.1}Ga_{0.8}As$	Spacer layer	20 nm
n+ GaAs	Base	1000 nm, $N_d = 2e17$
n+ GaAs	Buffer layer	500 nm, $N_d = 1e18$
Substrate GaAS n+		
Botton electrode		

Figure 1: The structure of MQW solar cell similar to the device reported in [5–7].

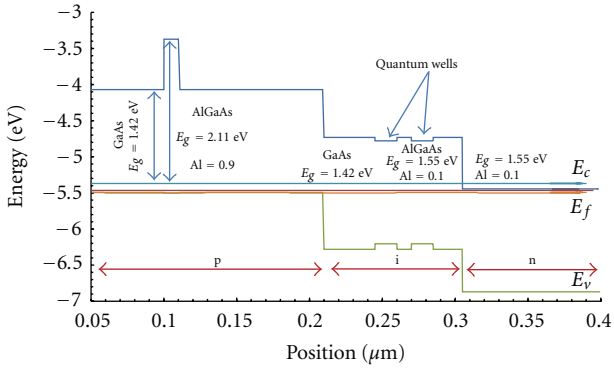

Figure 2: The energy band diagram of an optimized MQW cell.

and thicknesses at a center wavelength are designed for *GaAs* and for *AlAs*, respectively, discussed in the following. The energy band diagram of the DBR with 10 period used in this study is shown in Figure 3.

2. Device Modeling

Photogenerated electron hole pairs in semiconductors carry excess kinetic energy that is lost to the lattice by phonon emission. A photovoltaic MQW single junction device structure could take advantage of these high-energy carriers by allowing them to transport carriers across the semiconductor without being lost to the lattice through phonon scattering [9]. How useful one can design a MQW device, and to fully realize the potential of hot electron phenomena in confinement depends on an accurate modeling and design of the device. The energy balance modeling provides a relaxation lifetime for the energy transfer among the charge carriers and lattice. The solution of energy balance equation in single quantum well determines the average electron temperature and its relationship with the macroscopic energy relaxation lifetime assigned to hot electrons [10, 11]. The combination of multiple absorption and the confinement of hot electrons and the selective use of multiple DBR reflector for light trapping may further improve the efficiency of solar cells.

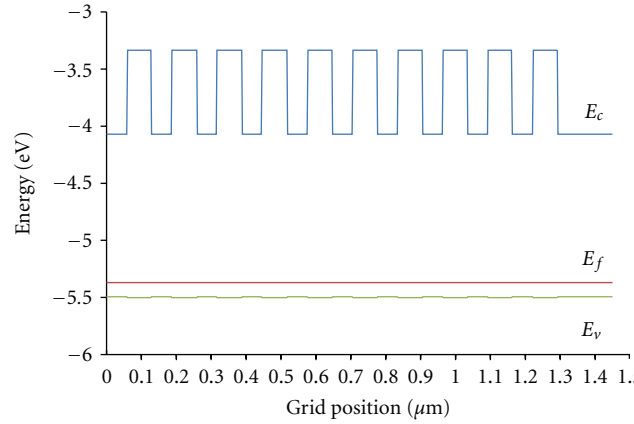

Figure 3: Energy band diagram of AlAs/GaAs DBR.

In the quantum well, the size quantization and the 2D density of states are applied. The electrons and holes energy levels in the well are estimated from the analytical expressions for a finite height well. Electron-hole generation due to optical absorption and generation-recombination due to Shockley-Read-Hall (SRH) and band-to-band radiative mechanisms are included. The generation-recombination terms in the bulk are modified and extended to quantum well regions. Energy transfer among the charge carriers and crystal lattice is modeled by an energy relaxation lifetime.

The kinetic energy for electrons (u_n) and holes (u_p) at a given temperature, $u_{n,p} = (3/2)k_B T_{n,p}$, is related by carrier temperature ($T_{n,p}$) and carrier populations, obtained by the interaction of carrier and phonon lattice. The kinetic energy exchange is modeled by $(u_{n,p}(T_{n,p}) - u_{n,p}(T_L))/\eta_{n,p}$ where the energy exchange among the lattice and carriers is modeled by energy relaxation lifetime for electrons (η_n) and energy relaxation lifetime for holes (η_p) discussed in [12, 13]. The parameter T_L is the lattice temperature and normally is kept at the nominal room temperature. The expression for the direct kinetic energy exchange among the electron and hole carriers is based on the effective mass approximation due to optical generation for electron and holes in the bulk described in detail in articles [14, 15]. The details of the device modeling and the formulations are also discussed in our previous work published in [16, 17].

2.1. Back Surface DBR Design. The efficiency of the AlGaAs/GaAs MQW can be increased by applying AlAs/GaAs distributed Bragg reflectors DBR at the back surface. The DBR also transmits the unabsorbed photons to be applied to a potential second cell attached to the bottom. This could potentially increase the open circuit voltage if a continuous current flow is maintained throughout the device. A DBR structure is formed from multiple layers of alternating materials with varying refractive index. Each layer boundary causes a partial reflection of an optical wave. The range of wavelengths that are reflected is called the photonic stopband. Also, most light outside of its stopband is transmitted through the cell. Therefore, a DBR structure is applied in

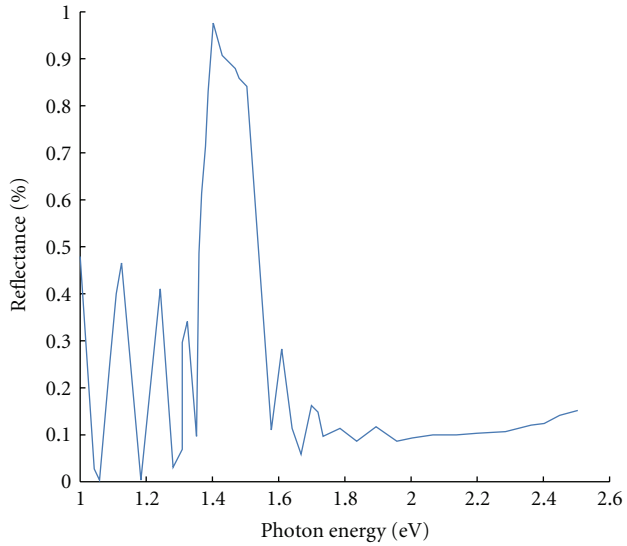

Figure 4: Reflectivity spectrum of AlAs/GaAs DBR versus photon energy.

order to reflect unabsorbed photons from the GaAs/AlGaAs QW junction.

To design a DBR that reflects unabsorbed photons from the MQW cell, the refractive index for GaAS and AlAs layers must be properly chosen for a particular wavelength. Thicknesses d_{Bragg} of Bragg reflectors layers were chosen in accordance with the following equation:

$$d_{\text{Bragg}} = \frac{\lambda}{4n_{\text{Bragg}}(\lambda)}, \tag{1}$$

where λ is the wavelength at maximum of spectral characteristic and n_{Bragg} is the refractive index for Bragg reflector material. Here, it is desired to reflect photons which have energies in the range between 1.4 ev and 1.6 ev. The refractive indexes and thicknesses for *GaAs* and *AlAs* layers at $0.88\,\mu$ are

$$n_1 = 3.662 \; d_1 = 0.05802\mu \text{ for } GaAs, \tag{2}$$

$$n_2 = 2.98581 \quad d_2 = 0.07116\mu \text{ for } AlAs. \tag{3}$$

An AlAs/GaAs DBR with a center wavelength at $0.88\,\mu$ is designed and simulated.

An AlAs/GaAs DBR with 10 periods is modeled at back surface of a MQW p-i-n cell. The simulation results indicate that the short-circuit current density of the QW cell increases by about 1 mA/cm^2 and the efficiency by 0.7% when applying the DBR. The reflectivity spectrum for the AlAs/GaAs DBR with 10 periods and the energy band diagram are illustrated in Figures 3 and 4. From Figure 3, it can be seen that the DBR has a high reflectance of about 1 between 1.4 ev and 1.6 ev and low reflectance at energies outside of the stopband.

2.2. AlGaAs/GaAs p-i-n Quantum Well: An Experimental Verification. The experimental AlGaAs/GaAs quantum well structure is an $Al_xGa_{1-x}As$ p-i-n with $x = 0.34$ containing a 145Å QW in the center of a $0.3\,\mu$m i layer. The thickness

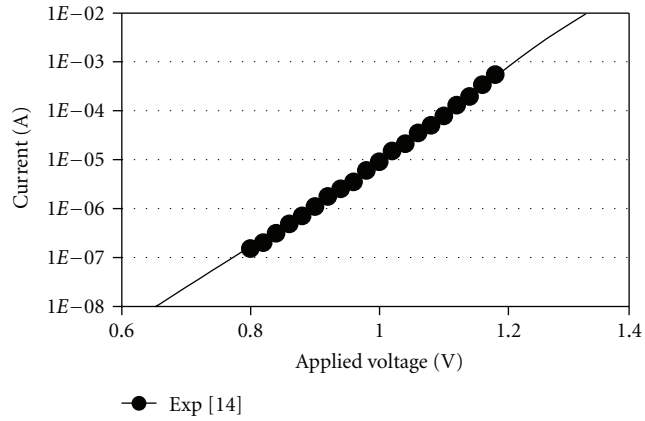

Figure 5: Simulated and measured dark current-voltage characteristics of a single QW $Al_{0.34}Ga_{0.66}As$/GaAs p-i-n cell. The measured data is taken from [14]. An energy relaxation of 1 ps and a SHR recombination of 1 ns are used.

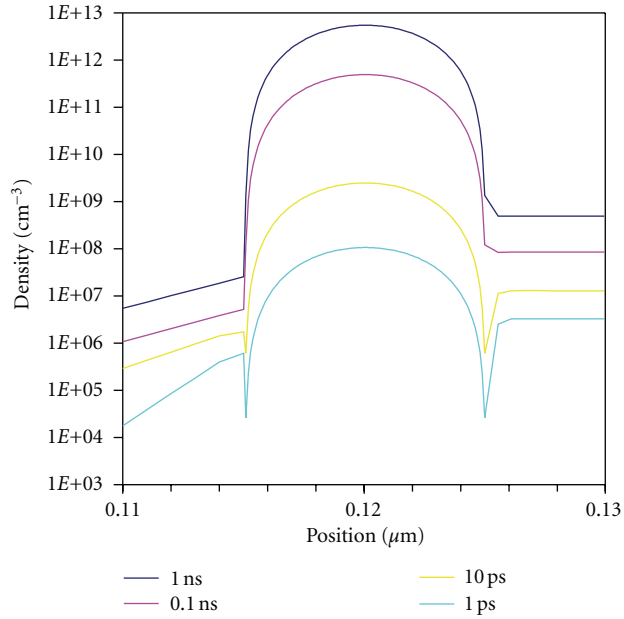

Figure 6: Simulated total electron density distribution in single QW as a function of energy relaxation lifetime at the forward bias of 1.3 V.

and the area of the p-i-n structure are $1.05\,\mu$m and 0.78 mm^2, respectively [14]. The p-type layer with the doping density of 2×10^{18} cm^{-3} and an n-type layer with the doping density of 2×10^{18} cm^{-3} are considered. A comparison between the simulation and experimental current-voltage characteristics of this device, Figure 5, shows that our model is capable of predicting the device current-voltage characteristics as well as giving physical insight into the device performance.

An energy relaxation lifetime of 1 ps is assumed. Not shown is the electron quantized energy level, calculated at 0.0254 eV above the conduction band. The temperature and total carrier concentration profiles are shown in Figures 6 and 7 at the forward bias of 1.3 V. The total carrier

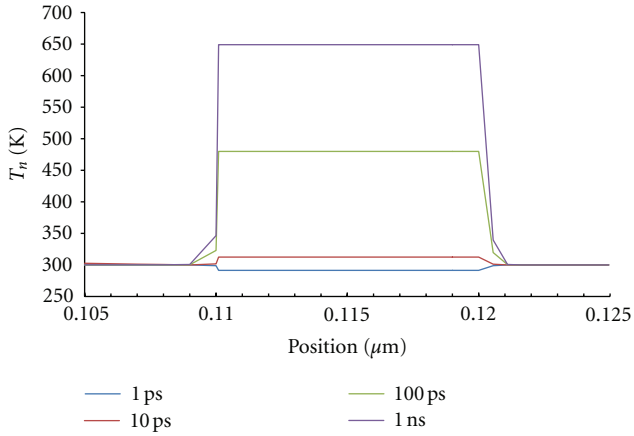

Figure 7: Average electron temperature distribution in single QW $Al_{0.34}Ga_{0.66}As$/GaAs p-i-n cell at different energy relaxation lifetime at the forward bias of 1.3 V.

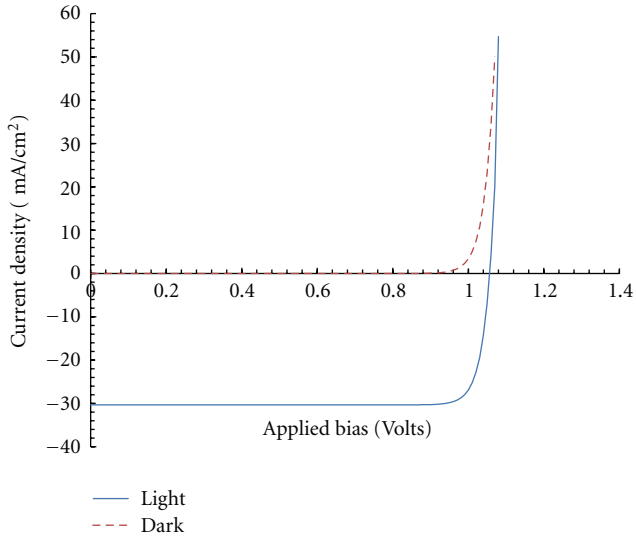

Figure 8: The I-V characteristic of the optimized AlGaAs/GaAs QW-DBR cell with and without light.

concentration includes both 2D bound and free carrier concentration. As shown, electrons transport away from the region with higher temperature due to thermal diffusion. The contacts are kept at lattice room temperature. The electron temperature rises in QW region, which has an energy relaxation lifetime of 1ps relative to the other regions in the semiconductor that were assumed to have much shorter energy lifetime. As a result electrons relax to lattice temperature outside the QW region.

2.3. AlGaAs/GaAs QW-DBR: An Optimized Device. The computed current-voltage characteristic of the optimized AlGaAs/GaAs QW-DBR structure described in Figure 1 with and without light is shown in Figure 8. A comparison between the AlGaAs solar cell with and without quantum wells is shown in Table 1. An open-circuit voltage of 1.06 Volt and a shortcircuit current density of 29.4 mA/cm^2 are obtained for the MQW cell. As shown in Table 1, MQW solar cells provide higher efficiency compared to their bulk p-n diode counterparts.

Table 1: Simulation results for different cells under AM1.5 spectrum.

	AlGaAs ($x = 0.1$) Bulk	AlGaAs ($x = 0.1$) MQW	AlGaAs (MQW) + DBR
J_{SC} (mA/cm^2)	29.2	29.4	30.3
V_{OC} (V)	1.03	1.06	1.06
$J_m \cdot V_m$ (mW/cm^2)	26.4	27.7	28.4

When the DBR is added to the MQW cell, the short-circuit current density increases by about 1 mA/cm^2 from 29.4 mA/cm^2, to 30.3 mA/cm^2, and the efficiency is increased by about 0.7%.

In summary, simulation results predict an efficiency of about 28.4% for the MQW *AlGaAs*-DBR single *p-i-n* junction photovoltaic cell under the presence of both radiative and nonradiative recombination mechanisms.

3. Conclusion

Simulation of MQW *AlGaAs* single p-i-n with back surface DBR is carried out by an energy balance modeling device simulation program under the AM 1.5 solar spectrum conditions. Results show that the quantum well solar cells can enhance short-circuit current and power conversion efficiency in comparison with similar, conventional solar cells made from bulk *AlGaAs* barrier material alone. 27.7% conversion efficiency was obtained by the MQW solar cell. The application of *AlAs/GaAs* DBRs at the back surface MQW increases the efficiency by about 1% with a total efficiency of 28.4%. The DBR structure reflects the part of the spectrum that benefits from absorption in the *AlGaAs* QW structure, while being transparent to the IR spectrum. The DBR can be used as a buffer to attach a second cell to absorb the transmitted photons for an increased efficiency if designed for a continuous current.

References

[1] J. G. J. Adams, W. Elder, G. Hill, J. S. Roberts, K. W. J. Barnham, and N. J. Ekins-Daukes, "Higher limiting efficiencies for nanostructured solar cells," in *Proceedings of the Physics and Simulation of Optoelectronic Devices XVIII*, vol. 7597 of *Proceedings of SPIE*, pp. 759705–759709, San Francisco, Calif, USA, January 2010.

[2] U. Aeberhard, "Microscopic theory and numerical simulation of quantum well solar cells," in *Proceedings of the Physics and Simulation of Optoelectronic Devices XVIII*, vol. 7597 of *Proceedings of SPIE*, pp. 759702–759712, San Francisco, Calif, USA, January 2010.

[3] K. Barnham, I. Ballard, J. Barnes et al., "Quantum well solar cells," *Applied Surface Science*, vol. 113-114, pp. 722–733, 1997.

[4] R. Corkish and C. B. Honsberg, "Dark currents in double-heterostructure and quantum-well solar cells," in *Proceedings*

of the 26th IEEE Photovoltaic Specialists Conference, pp. 923–926, October 1997.

[5] J. Prazmowska, R. Korbutowicz, R. Paszkiewicz, and M. Tlaczala, "Parameters comparison of p-i-n and quantum well solar cells," *Optica Applicata*, vol. 37, no. 4, pp. 371–376, 2007.

[6] J. Prazmowska, R. Paszkiewicz, R. Korbutowicz, M. Wośko, and M. TŁaczałA, "Solar cells conversion efficiency enhancement techniques," *Optica Applicata*, vol. 37, no. 1-2, pp. 93–99, 2007.

[7] J. Prazmowska and R. Korbutowicz, "Optimization of multi quantum well solar cell," *Optica Applicata*, vol. 35, no. 3, pp. 619–626, 2005.

[8] S. M. Sze and K. K. Ng, *Physics of Semiconductor Devices*, Wiley-Interscience, Hoboken, NJ, USA, 2007.

[9] M. A. Green, K. Emery, Y. Hishikawa, and W. Warta, "Solar cell efficiency tables (Version 33)," *Progress in Photovoltaics*, vol. 17, no. 1, pp. 85–94, 2009.

[10] M. D. Kelzenberg, D. B. Turner-Evans, B. M. Kayes et al., "Photovoltaic measurements in single-nanowire silicon solar cells," *Nano Letters*, vol. 8, no. 2, pp. 710–714, 2008.

[11] T. J. Kempa, B. Tian, D. R. Kim, J. Hu, X. Zheng, and C. M. Lieber, "Single and tandem axial p-i-n nanowire photovoltaic devices," *Nano Letters*, vol. 8, no. 10, pp. 3456–3460, 2008.

[12] M. Paxman, J. Nelson, B. Braun et al., "Modeling the spectral response of the quantum well solar cell," *Journal of Applied Physics*, vol. 74, no. 1, pp. 614–621, 1993.

[13] Y. Rosenwaks, M. C. Hanna, D. H. Levi, D. M. Szmyd, R. K. Ahrenkiel, and A. J. Nozik, "Hot-carrier cooling in GaAs: quantum wells versus bulk," *Physical Review B*, vol. 48, no. 19, pp. 14675–14678, 1993.

[14] J. Nelson, J. Barnes, N. Ekins-Daukes et al., "Observation of suppressed radiative recombination in single quantum well p-i-n photodiodes," *Journal of Applied Physics*, vol. 82, no. 12, pp. 6240–6246, 1997.

[15] D. Chen, Z. Yu, K. C. Wu, R. Goosens, and C. W. Dutton, "Dual energy transport model with coupled lattice and carrier temperatures," in *Proceedings of the 5th SISDEP Conference*, pp. 157–160, Vienna, Austria, September 1993.

[16] H. Z. Fardi, D. W. Winston, R. E. Hayes, and M. C. Hanna, "Numerical modeling of energy balance equations in quantum well $Al_xGa_{1-x}As$/GaAs p-i-n photodiodes," *IEEE Transactions on Electron Devices*, vol. 47, no. 5, pp. 915–921, 2000.

[17] H. Z. Fardi, "Detailed formulation of energy balance equations in single quantum well devices," *COMPEL*, vol. 21, no. 3, pp. 425–437, 2002.